

Surface interpolation and 3D relatability

Carlo Fantoni

Department of Psychology and B.R.A.I.N. Center for Neuroscience, University of Trieste, Trieste, Italy, & Department of Neuroscience and Cognitive Systems, Italian Institute of Technology, Parma, Italy



James D. Hilger

Department of Psychology, University of California, Los Angeles, CA, USA



Walter Gerbino

Department of Psychology and B.R.A.I.N. Center for Neuroscience, University of Trieste, Trieste, Italy



Philip J. Kellman

Department of Psychology, University of California, Los Angeles, CA, USA



Although the role of surface-level processes has been demonstrated, visual interpolation models often emphasize contour relationships. We report two experiments on geometric constraints governing 3D interpolation between surface patches without visible edges. Observers were asked to classify pairs of planar patches specified by random dot disparities and visible through circular apertures (aligned or misaligned) in a frontoparallel occluder. On each trial, surfaces appeared in parallel or converging planes with vertical (in Experiment 1) or horizontal (in Experiment 2) tilt and variable amounts of slant. We expected the classification task to be facilitated when patches were perceived as connected. We found enhanced sensitivity and speed for 3D relatable vs. nonrelatable patches. Here 3D relatability does not involve oriented edges but rather inducing patches' orientations computed from stereoscopic information. Performance was markedly affected by slant anisotropy: both sensitivity and speed were worse for patches with horizontal tilt. We found nearly identical advantages of 3D relatability on performance, suggesting an isotropic unit formation process. Results are interpreted as evidence that inducing slant constrains surface interpolation in the absence of explicit edge information: 3D contour and surface interpolation processes share common geometric constraints as formalized by 3D relatability.

Keywords: completion, surface, amodal, modal, relatability, interpolation, 3D, disparity, stereopsis

Citation: Fantoni, C., Hilger, J. D., Gerbino, W., & Kellman, P. J. (2008). Surface interpolation and 3D relatability. *Journal of Vision*, 8(7):29, 1–19, <http://journalofvision.org/8/7/29/>, doi:10.1167/8.7.29.

Introduction

Since light moves in straight lines, optic information about opaque objects is fragmentary (Kanizsa, 1979; Kellman & Shipley, 1991; Koffka, 1935; Marr, 1982; Metzger, 1954; Michotte, Thinès, & Crabbé, 1964). Therefore, the following problem arises: How does the visual system connect spatially separate fragments to generate unitary visual shapes that adequately represent physical objects?

Achieving such representations places demands on both information extraction and computation. The visual system must connect visible fragments and *fill in gaps* (Ullman, 1976). Visual interpolation seems to result in representation of units with continuous contours and surfaces.

Although processes uniquely involved with surface information have been demonstrated (Albert, 2001; Fantoni, Bertamini, & Gerbino, 2005; Tse & Albert, 1998; Yin, Kellman, & Shipley, 1997, 2000), interpolation models have more thoroughly described contour relationships (Field, Hayes, & Hess, 1993; Fulvio, Singh, &

Maloney, 2008; Geisler, Perry, Super, & Gallogly, 2001; Heitger, Rosenthaler, von der Heydt, Peterhans, & Kübler, 1992; Heitger, von der Heydt, Peterhans, Rosenthaler, & Kubler, 1998; Singh & Hoffman, 1999; Takeichi, Nakazawa, Murakami, & Shimojo, 1995). *Contour interpolation* is conceived as the connection of *inducing contours* through smooth (differentiable at least once) monotonic paths, taking edges and tangent discontinuities (end-points and junctions) as the input. In complementary fashion, *surface interpolation* is conceived as a spreading of feature-specific activation within bounded regions or as an unconstrained flow of feature-specific activation when edge information is missing (Kellman, 2003; Yin et al., 2000).

Figure 1 demonstrates how *surface linking* (as discussed by Yin et al., 1997) relates to edge geometry and color similarity in 2D displays. Whereas the blue disk on the upper right appears as a figure on the gray background, being located outside the amodal boundaries of the partially occluded shape, other blue disks appear as holes, being located inside such boundaries. Color

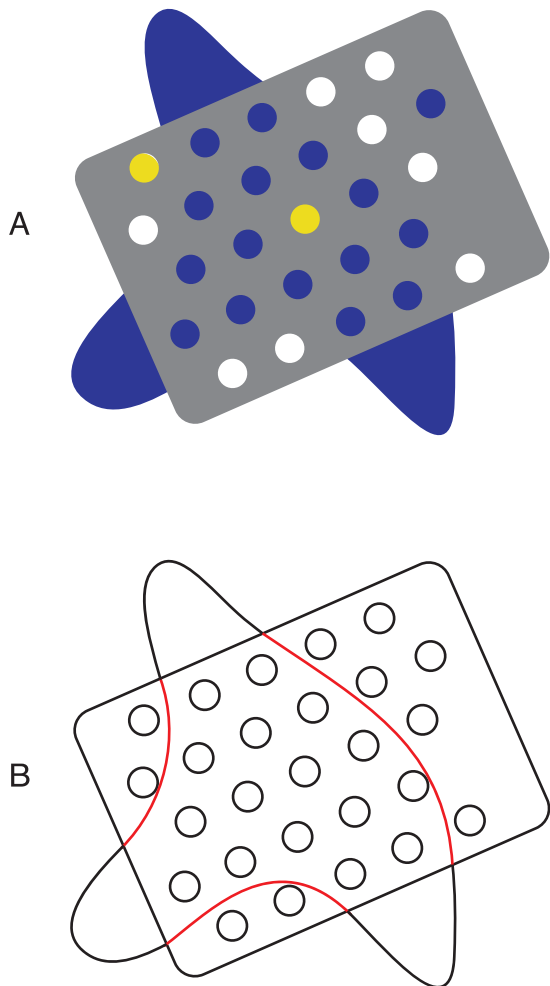


Figure 1. (A) Surface completion in 2D. (B) Amodal boundaries generated by contour interpolation (in red). The blue disks within amodal boundaries appear as holes unified with the three blue protrusions. The blue disk outside the amodal boundaries and the yellow disks appear as occluding spots. White disks outside amodal boundaries are seen as holes.

similarity explains why the yellow disks are segregated and appear as superposed figures, while the white disks always appear as holes revealing part of the background, regardless of the lack of tangent discontinuities that are ordinarily required to trigger contour interpolation process.

Prior work focused on pictorial displays (in which surface fragments were necessarily coplanar) and thus could not reveal the role of geometric relations between inducing surface patches. We reasoned that 3D interpolation might reveal the role of surface-level geometric constraints, similar to those for both 2D and 3D contour interpolation. The 3D positions and orientations of unbounded patches may constrain their connection to form 3D amodal surfaces. In this research, we sought to discover whether geometric constraints govern the interpolation of textured patches in the absence of explicit contour information.

Geometric constraints on contour interpolation have been studied extensively. Few studies have specifically focused on surface interpolation, as when two holes reveal patches of partially occluded surfaces (Figure 2). Saidpour, Braunstein, and Hoffman (1992, 1994) used structure from motion displays that simulated two converging random dot planes separated by a gap and found evidence that observers perceive a smooth 3D surface connecting the patches. Grimson (1981) included geometric constraints in an algorithm that locally interpolated a sample of points with depth values specified by disparity. Fantoni, Hilger, Gerbino, and Kellman (2005; Hilger, Fantoni, Gerbino, & Kellman, 2006) used patterns like those shown in Figure 2 to demonstrate that 3D surface interpolation is geometrically constrained. In Figure 2A, a vivid impression of surface completion arises from two patches that can be connected by a monotonic surface. In contrast, two unconnected surface patches are perceived in Figure 2B, where the two patches are offset in depth.

In the present experiments, we used displays similar to those in Figure 2 and found geometric constraints at the surface level similar to those found by Kellman, Garrigan, Shipley, Yin, and Machado (2005) for 3D interpolation at the contour level. As background, in the next section we describe relevant evidence and models concerning visual completion of contours and surfaces in both 2D and 3D cases.

Input and constraints for visual interpolation

In recent years, *contour relatability* (Kellman & Shipley, 1991) has served as a convenient way to formalize the geometric constraints for 2D contour completion because of its simplicity and consistency with empirical findings (Field et al., 1993; Fiorani, Rosa, Gattas, & Rocha-Miranda, 1992; Gerbino & Fantoni, 2006; Guttman, Sekuler, & Kellman, 2003; Kellman & Shipley, 1991; Li & Li, 1994; Ringach & Shapley, 1996).

Two contour fragments are relatable when their connection bends in only one direction (*monotonicity constraint*) through an obtuse angle (*90-deg constraint*). As shown in Figure 3, formally the $[0 \leq R\cos(\tau) \leq r]$ inequality (with R and r normal to the junction stems, $R \geq r$, and the τ angle formed by their intersection) must be satisfied for contour completion to take place. This principle implies two basic types of relatability violations: *type I* ($R\cos(\tau) \geq r$) when two fragments are misaligned along the bisector of the interpolation angle and their smooth connection would require the generation of a nonmonotonic trajectory; and *type II* ($R\cos(\tau) \leq 0$) when two fragments are tilted in opposite directions so that their linear extrapolations form an obtuse angle.

Surface and contours in 2D interpolation

It has been suggested that contour interpolation and surface interpolation processes may be complementary, with

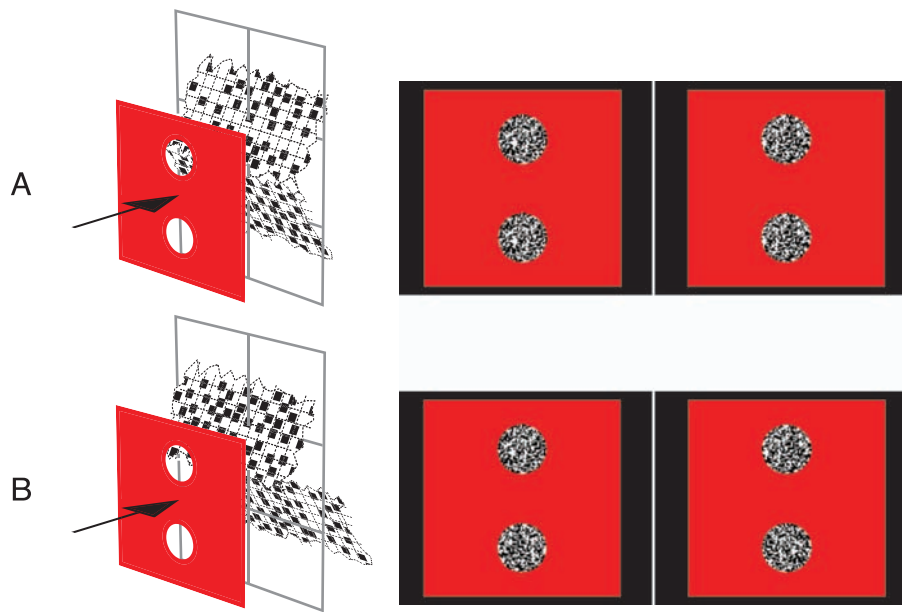


Figure 2. Two stereograms used by Fantoni, Hilger et al. (2005) and Hilger et al. (2006) to demonstrate the occurrence of visual completion in the absence of explicit edge information. (A) A unitary monotonic surface connecting the two random dot patches is perceived. (B) Where a depth offset separates the two patches, they are perceived as unconnected surfaces. A 3D view of the simulated patterns is shown on the left (the arrow indicates the cyclopean visual axis).

surface spreading occurring within given or interpolated object boundaries (Grossberg & Mingolla, 1985; Kellman & Shipley, 1991; Nakayama, Shimojo, & Silverman, 1989). Studies by Yin et al. (1997, 2000) provided evidence of objective performance effects from surface completion processes, exhibiting a dependence on the

presence of surface similarity, as well as an interaction with boundary completion processes. Yin et al. (1997) found that a small circular region on a surface occluding two bars is more likely to be judged as a hole (rather than a spot) when it shares identical surface properties to the bars and is within relatable edges. In a subsequent work,

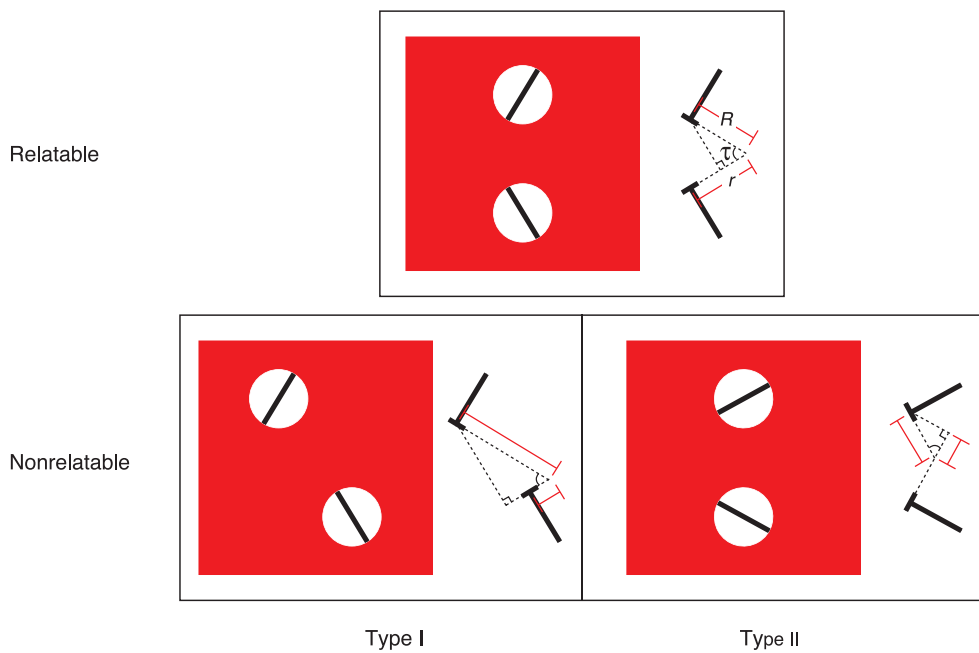


Figure 3. Geometry of contour relatability and of its basic violations. Contour relatability between fragments centered on white circular regions and tilted in opposite directions (top row) is violated in two ways (bottom row): (1) relative shift between visible contour fragments (Type I); (2) orientation of fragments such that their linear extrapolations form an obtuse angle (Type II).

Yin et al. (2000) found evidence that the interplay between contour and surface completion operates across varying depths. The authors used displays similar to those of Yin et al. (1997) and found that under conditions where surface interpolation would be expected, sensitivity to depth given by disparity is systematically altered.

3D contour relatability

Kellman, Garrigan, and Shipley (2005) generalized theoretical work on 2D contour interpolation to construct a more general theory of 3D contour interpolation. Each inducing edge at a tangent discontinuity (contour junction) is represented by a 3D *orientation vector* and a 3D *position vector*, once a coordinate system is provided. 3D relatability imposes constraints of smooth, monotonic contour connections in 3D. Intuitively, this can be understood as requiring the inducing edges to lie (approximately) in some plane in 3D space, and within that plane, the edges must fulfill the original 2D relatability criteria. Interpolated surfaces given by 3D relatability cannot include inflections, torsion, and cannot bend through more than 90 deg.

Kellman, Garrigan, Shipley, Yin et al. (2005) tested the theory of 3D relatability in a series of experiments. As it is similar to the one we used in our experiments, we describe their objective performance task in some detail.

Observers were asked to judge on each trial whether a pair of inducing planar surface patches had either parallel or converging orientations in 3D space. Half of the parallel and half of the converging displays fit the criteria of 3D relatability being connectable in depth by a monotonic curve. In contrast to the displays shown in Figure 2 and used throughout our experiments, their

displays (Figure 4) involved modal completion (instead of amodal) and included bounded surfaces as inducing elements (instead of unbounded). Analogous to a number of paradigms used in 2D object formation (e.g., Baylis & Driver, 1993; Behrmann, Zemel, & Mozer, 1998; Duncan, 1984; Gold, Murray, Bennet, & Sekuler, 2000; Kramer & Watson, 1996; Ringach & Shapley, 1996; Sekuler, Palmer, & Flynn, 1994), it was hypothesized that object formation would produce a performance advantage for the classification task. Results showed large advantages in sensitivity and response time for 3D relatable displays. A number of control conditions indicated that the performance advantages depended on 3D object formation mediated by 3D relatability and not on the specific aspects of the geometric relations between inducers such as the depth offset or their relative orientation.

Surfaces and contours in 3D interpolation

Two of the studies of Kellman, Garrigan, Shipley, Yin et al. (2005) provided evidence that contour interpolation, not surface interpolation, produced the 3D relatability advantage. The performance advantage was eliminated when the edges of surface patches were rounded or when their lateral misalignment was large: both of these manipulations are known to disrupt contour relatability but not the 3D surface geometry characteristic of relatable displays. Those studies, however, did not fully explore the performance effects of surface interpolation. Specifically, the displays of Kellman, Garrigan, Shipley, Yin et al. (2005) contained a conflict: they were cases in which contour information did not support surface interpolation.

In the present work, we examined situations that allow more straightforward examination of surface processes.

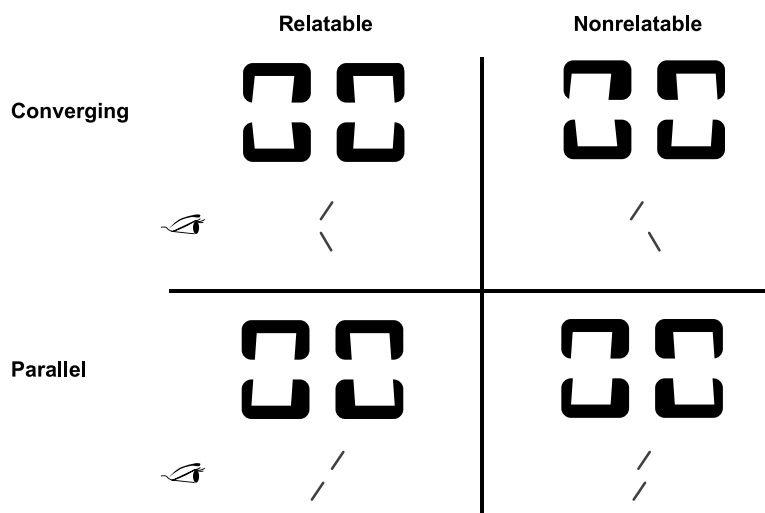


Figure 4. Example of the displays used by Kellman, Garrigan, Shipley, Yin et al. (2005) to test the effect of 3D contour relatability on the speeded classification of parallel/converging displays (rows) either relatable or not (columns). In each quadrant, the upper image is a stereo pair of the two illusory planes slanted in depth, and the lower image is a side view of the same planes [redrawn with permission from Kellman, Garrigan, Shipley, Yin et al. (2005)].

We used stereoscopic surface patches that contained no contour information (as those of Figure 2). These displays allowed us to test whether the 3D relatability constraints apply even in the absence of any explicit edge information. We reasoned that in 3D, it would be odd if there were no geometric constraints on surface interpolation, and we hypothesized that surface interpolation might follow geometric constraints similar to those for 3D contour interpolation.

Elaborating such a hypothesis requires identifying the initiating conditions for 3D *surface interpolation*. The orientation and position of inducing surface patches are likely to be important, and these must somehow be extracted from the distribution of projected surface markings (Knill, 1992; Stevens, 1981, 1983).

Figure 5 shows that, in a viewer centered coordinate system, the orientation of a stereoscopic planar surface patch can be parametrized, according to Gibson (1950), by the magnitude of *slant* (angle between the surface normal and the visual axis) and by the direction of slant or *tilt* (angle between the projection of the surface normal in the image plane and the horizontal axis). For instance, surfaces slanting with the same angle but around opposite axes (Figure 5, from left to right, around the *x* and *y* axes, respectively) have orthogonal tilt directions (vertical and horizontal, respectively) involving different horizontal transformations between the two monocular images (horizontal shear and scale, respectively).

Whether the extraction of stereoscopic planar surface orientation is achieved either indirectly, mapping of small positional disparities (zero order) between corresponding points in the two monocular images into a depth map (Blake & Zisserman, 1987; Grimson, 1981; Marr & Poggio, 1979; Terzopoulos, 1986) or directly, picking-up

projective invariants embodied in the distribution of higher order disparity, such as disparity gradients, orientation, and horizontal size disparity, is still a matter of debate (Blakemore, 1970; Gårding, Porritt, Mayhew, & Frisby, 1995; Gibson, 1950, 1979; Howard & Kaneko, 1994; Jones & Malik, 1991; Koenderink & van Doorn, 1976; Malik & Rosenholtz, 1997; Mayhew & Longuet-Higgins, 1982; Nguyenkim & DeAngelis, 2003; Tyler & Sutter, 1979; van Ee & Erkelens, 1998; Wildes, 1991).

The aim of most indirect models is the recovery of a description of the object (by means of the smooth interpolation of the sparse field of point disparities) that best approximates its distal geometry: ideally a Euclidean copy (up to a scale factor). However, evidence reviewed by Domini and Caudék (2003) suggests that perceived 3D structures are neither Euclidean nor affine. In particular, several studies (Bradshaw & Rogers, 1993; Caganelli & Rogers, 1988, 1993; Fantoni & Gerbino, 2006; Gillam, Flagg, & Finlay, 1984; Gillam & Ryan, 1992; Mitchison & McKee, 1990; van Ee & Erkelens, 1995; Wallach & Bacon, 1976) found *slant anisotropy*; i.e., lower detection threshold and faster resolution for the slant of planes with vertical rather than horizontal tilt. In accordance with Rogers and Graham (1983) slant anisotropy can be directly explained by the arrangement of higher order disparity embodied in the two monocular images of planes with the same slant but orthogonal tilt directions. Indeed, horizontal shear and scale transformations generate gradients of horizontal disparity that are in orthogonal directions, as well as patterns of orientation disparity with different magnitudes (with a larger orientation disparity generated by a horizontal shear rather than scale transformation).

We speculated that a direct specification of surface orientation (rather than a demanding indirect reconstruction)

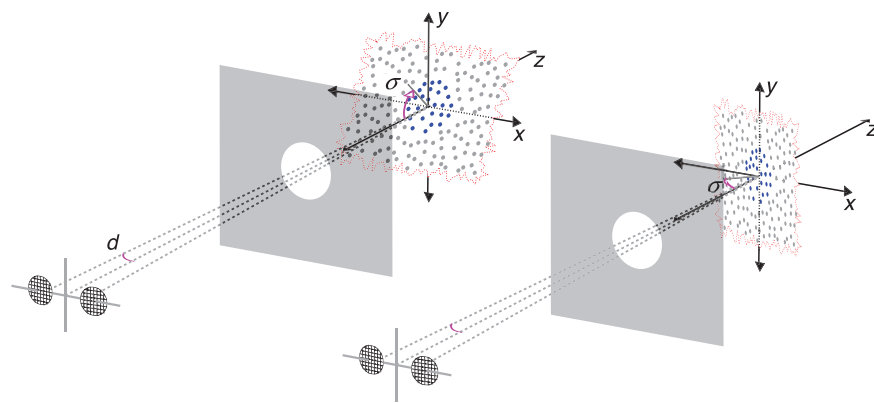


Figure 5. Two planar surface patches viewed through a circular aperture on a screen, with the same slant angle (σ) but orthogonal tilt directions (vertical and horizontal from left to right), as depicted by the pink arcs connecting the solid cylinder stacked on the center of the surface with the *z* axis. Planar surface orientation is coded in a viewer centered coordinate system, where the *x*, *y*, and *z* axes are defined on the basis of the viewing geometry as described by: two gray ellipses (representing the two eyes), converging (with an angle d) on the planar surface center; a cyclopean line of sight that is the line that connects the midpoint between the eyes and the fixation point and that is aligned and centered with the *z* axis; the interocular axis that is the line passing through the two ellipse centers that is parallel to the *x* axis; and a line through the point midway between the two eyes and orthogonal to both the interocular axis and the cyclopean line of sight that is parallel to the *y* axis.

may be more likely to constitute the base input for early processing involved in visual completion of surface and contours (for a discussion see Kellman, Guttman, & Wickens, 2001). Recent computational models provide useful insights on how to optimize the 3D shape from disparity process through combining position with different types of higher order disparities (Jones & Malik, 1991; Li & Zucker, 2005). Current works on neural loci relevant to visual interpolation (Bakin, Nakayama, & Gilbert, 2000; Kapadia, Ito, Gilbert, & Westheimer, 1995; Moore & Engel, 2001; Murray, Foxe, Javitt, & Foxe, 2004) do not provide information on the type of disparity (zero order vs. higher order) used in the perception of inducing surface orientation. This question might be answered psychophysically, in part by looking for slant anisotropy in visual interpolation.

Experiments 1 and 2

In two experiments, we tested whether 3D surface interpolation aids the classification of pairs of converging/parallel planar surface patches (Aim #1), whether its classification effects are isotropic over different global orientations of the inducing surfaces (Aim #2), and whether there is an anisotropy in the perception of inducing surfaces

slant as expected on the basis of the different pattern of higher order disparities generated by inducing surfaces with a vertical vs. horizontal tilt direction (Aim #3).

Summary of experiments and hypotheses

These aims were assessed by measuring the observers' sensitivity and response time to perform a speeded classification task where they were required to identify whether a pair of patches was parallel or converging. This task was done both for pairs of *3D relatable* (i.e., connectable by a smooth monotonic surface) and *3D nonrelatable* (i.e., not connectable by a smooth monotonic surface) patches with variable slant and orthogonal tilt direction (i.e., vertical in Experiment 1 and horizontal in Experiment 2), visible through pair of apertures that were *aligned* or *misaligned* relative to the direction of tilt of the inducing surfaces.

In both experiments, pairs of converging/parallel inducing planar surface patches were presented in 20 spatial conditions. Experimental factors were: *3D relatability* of the inducing surfaces (3D relatable vs. 3D nonrelatable); *alignment* of the aperture pair (aligned vs. misaligned), absolute *inducing surface slant* ($\theta = 20, 35, 46, 54, 60$ deg). Figure 6 summarizes the experimental set of displays used in Experiments 1 and 2. According to this design, surface patches could violate relatability

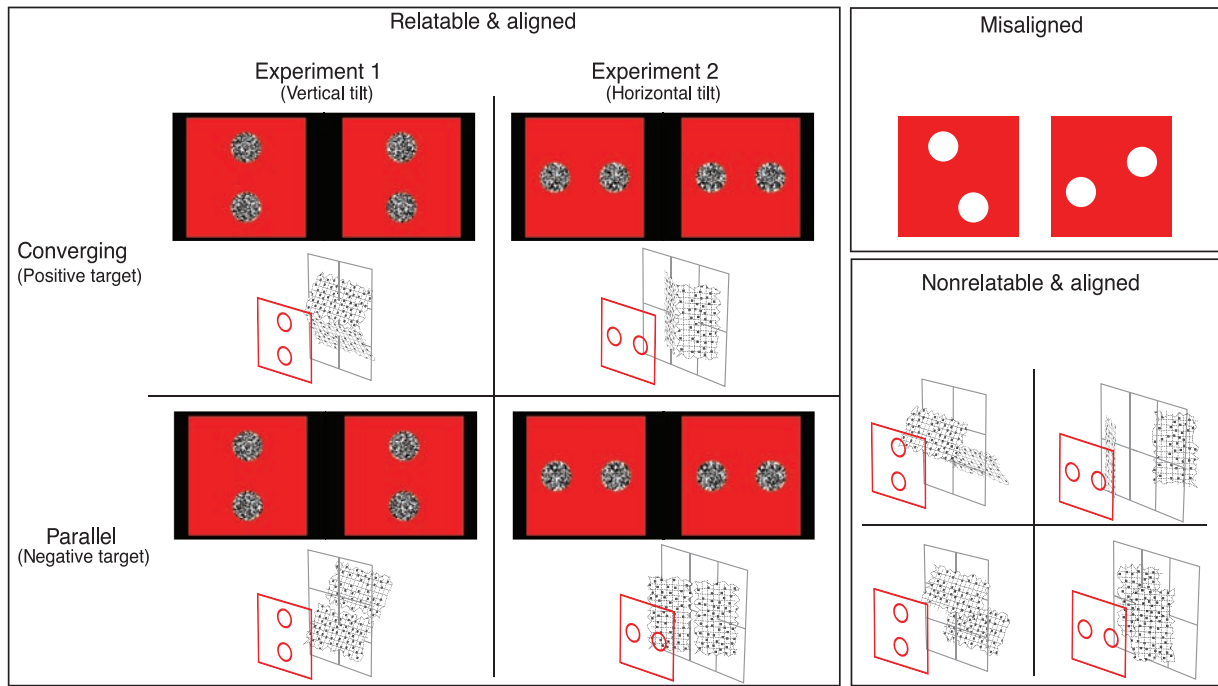


Figure 6. Summary of the experimental set used in Experiments 1 and 2 for the 46-deg inducing surface slant condition. The left box depicts 3D relatable with aligned aperture displays with display type (converging/parallel) in rows and the global orientation of inducers (vertical/horizontal tilt direction) in columns. In each quadrant of the box, the upper image is a stereo pair of 3D relatable inducing surfaces and the lower image is a 3D view of the same surfaces. In the bottom/right box, a similar 3D view is provided for 3D nonrelatable displays with aligned apertures. The top/right box shows misaligned apertures for Experiment 1 (left) and Experiment 2 (right).

constraints in two ways. The first involved shifting relatable surface patches in opposing directions in depth so that a monotonic connection would be impossible. The second involved the use of slant magnitudes that implied (in the case of converging displays) a connecting surface bending through an angle smaller than 90 deg. The label “3D relatable” is used for clarity in connecting the stimuli to the hypotheses and for consistency with prior work (Kellman, Garrigan, & Shipley, 2005; Kellman, Garrigan, Shipley, Yin et al., 2005). We note, however, that strictly speaking converging displays with inducing surface slant larger than 45 deg (i.e., 46, 54, 60 deg) were nonrelatable because they violated the 90-deg constraint. The effects of these larger slants in the data are discussed below.

With regards to Aim #1, consistent with Kellman, Garrigan, Shipley, Yin et al. (2005), we expected that 3D relatability would produce an advantage in speeded classification performance with a global improvement for relatable over nonrelatable displays. While classification performance should improve as simulated slant increases regardless of the relatability between inducing surface patches (Braunstein, 1968; Harris, Freeman, & Hughes, 1992), it should improve more dramatically for relatable displays and thus exhibit different sensitivity/RT functions than those stemming from nonrelatable displays. This difference would be independent of any effect stemming from slant sensitivity alone and would thus likely result from the depth offset (i.e., 3D relatability) of the two surface patches. Furthermore, an inducing surface slant \times 3D relatability interaction with decreasing advantage for relatable over nonrelatable displays as surface slant increases beyond 45 deg would be consistent with the operation of the 90-deg constraint. We expected that such an interaction might be most noticeable on the RT measure (the sensitivity measure inherently combines converging and parallel as the two response options and the 90-deg constraint arises only for converging displays). In sum, a full 3D relatability effect (i.e., involving the effect of both geometric constraints) would consist of a trade-off between simulated slant and performance advantage (for relatable vs. nonrelatable displays), with a decreasing advantage as slant increases.

The purpose of the aperture alignment factor was to investigate whether surface interpolation depends (besides on the slant) on the position of inducing surfaces in the image plane (that actually corresponds to that of the apertures) relative to their tilt direction. Indeed, in our displays the direction of tilt of inducing surfaces matches with the direction of the axis through the centers of aligned apertures (that was vertical in Experiment 1 where the tilt was vertical; and horizontal in Experiment 2 where the tilt was horizontal) but not with the one of misaligned apertures (that was oblique). However, in terms of 3D relatability, which depends on slant relations of the inducing surfaces (not the relative position of apertures), there are no obvious reasons to expect an advantage for displays with aligned apertures.

Aims #2 and #3 were assessed by comparing the classification data in Experiments 1 vs. 2. Both aims were fundamental to reveal the processes driving surface interpolation, including the coding of orientations of inducing surfaces and the generation of a connecting surface. Slant anisotropy (see [Surfaces and contours in 3D interpolation](#) section) could affect the coding of orientations of inducing surfaces in two ways:

1. By reducing the effectiveness of surfaces with horizontal vs. vertical tilt as inducers of a 3D percept. This would cause an overall increased difficulty in performing the classification task in Experiment 2 relative to Experiment 1, producing a main effect for the type of experiment;
2. By reducing the magnitude of perceived slant for inducing surface patches with horizontal relative to vertical tilt. This would cause the performance advantage due to 3D relatability to hold for a larger range of simulated slant values in Experiment 2 relative to Experiment 1.

Several studies suggest that the anisotropy is not limited to the coding of 3D planar surface orientation but rather to the coding of 3D surface structures (Cornilleau-Pérès & Droulez, 1989; Norman & Lappin, 1992; Rogers & Graham, 1983), with better perception of metric and structural attributes (i.e., curvature, depth, orientation) for simulated 3D objects (i.e., planes, cylinder, dihedral angle) whose global orientation involves a vertical rather than a horizontal tilt direction. We speculated that such higher order anisotropy could affect the unit formation process reducing the likelihood of the formation of 3D amodally completed structures including visible patches with horizontal relative to vertical tilt. This would cause a stronger performance advantage for relatable over non-relatable displays in Experiment 1 relative to Experiment 2, producing an experiment \times 3D relatability interaction.

In contrast, no substantial difference between the two experiments would suggest that both the processes involved in generating interpolated surfaces, and the coding of inducing surfaces’ orientation are isotropic.

In sum, the difference between Experiments 1 and 2 involved the global orientation of simulated 3D displays. The displays in Experiment 2 were 90-deg rotated copies (around the viewing axis) of those in Experiment 1. Other features of the displays were identical between the two experiments. For brevity, we describe the general method used in both Experiments 1 and 2, pointing out differences as necessary.

General method

Participants

Sixty-five UCLA students with normal or corrected-to-normal vision and naive to the purpose of the experiment

received class credit for participation in a 90-minute individual session. Thirty-five participated in Experiment 1, and thirty participated in Experiment 2. Three participants were omitted from Experiment 1 and six from Experiment 2 because they failed the test for stereoscopic slant perception (see *Procedure* section). Six of the thirty-two observers who completed Experiment 1 and six of the twenty-four observers who completed Experiment 2 were excluded from the final analysis due to failure to meet the threshold criterion for performance in the experimental task (average individual scores were required to fall between the 1.96 and $-1.96 z$ points). Each observer participated in all conditions of the factorial within-subjects designs.

Apparatus and displays

Stimuli were generated on a Macintosh G4 computer and displayed on a ViewSonic monitor measuring 21 in. diagonally (20 in. viewable) with a resolution of 1024×768 pixels at 140 Hz. Displays were disparate (top/bottom) images viewed with the use of liquid-crystal-diode (LCD) shutter glasses (Crystal EyesTM), synchronized to the monitor such that the shutter over each eye was opened electronically while the appropriate image for that eye was displayed on the monitor. The effect of interleaving the top and bottom images was that effective vertical resolution and refresh rate were halved (384 pixels at 70 Hz).

At a distance from the screen of 120 cm, 1 pixel subtended 1.14 arcmin and the visible area of the CRT screen subtended 18.7 deg horizontally and 14.3 deg vertically.

The computer associated a (for converging) and l (for coplanar) keys to each allowed response and recorded response type and reaction time (RT) using Matlab PsychToolbox functions (Pelli, 1997).

Left/right monocular images when fused defined a square-shaped frontoparallel occluder (5.67-deg extent) that had the following properties:

1. centered and orthogonal to the cyclopean line of sight;
2. staked out from the screen [18.2 arcmin of horizontal crossed disparity];
3. surrounded by a black background filling in the entire CRT screen;
4. with two 1.42-deg diameter circular apertures on it, each revealing a patch of a slanted surface covered by a uniform distribution (i.e., 50% density) of square black and white texture elements (3.41-arcmin extent).

Depending on the alignment condition, the two apertures could be: *aligned* relative to the vertical axis (in Experiment 1) or horizontal axis (in Experiment 2) through the center of the occluder; *misaligned* in opposite directions. In

misaligned displays, the center of each aperture deviates from the vertical/horizontal axis centered on the occluder by 0.71 deg with each aperture deviating in opposite directions for a total center-to-center misalignment of 1.42 deg (equal to the aperture diameter). The direction of misalignment was counterbalanced over our displays.

Side views or overhead views of the 3D stimuli used in Experiment 1 or 2, respectively, are shown in Figure 7. Simulated planar surface patches could be on either parallel planes (top and bottom surfaces having the same slant directions and magnitudes) or converging planes (top and bottom surfaces slanted in opposite directions). Orthographic projections and no lighting sources were used to minimize the monocular cues for 3D orientation. Figure 7 shows that nonrelatable displays (red lines) were created by shifting in depth the relatable surface patches (black lines) in opposite directions (each by the same amount). Taking the radius of an individual aperture as a reference size (i.e., 1), this corresponded to a constant 2 unit back/forth simulated depth shift of the top/bottom 3D relatable planar surfaces, while keeping the occluder plane at a constant 9 units distance from the center of the farther 3D relatable surface patch (corresponding to screen depth level, i.e., the point with zero horizontal disparity).

Across all nonrelatable displays, the sign of depth shift could either be positive (with the top planar surface shifted away from the observer) or negative (vice versa). Given that converging planes might be confused with parallels (if small converging slant are underestimated) while the opposite would be improbable, we chose the type of convergence that should favor depth perception: convex displays that converge toward the observer, in accordance with the results of several studies (Bertamini, 2001; de Vries, Kappers, & Koenderink, 1993, 1994; Hoffman & Richards, 1984; Liu & Todd, 2004). This was done to avoid any effect on performance stemming from whether interpolated surfaces were perceived as concave vs. convex. The overall sign of slant of parallel displays was either positive (slanting toward the observer) or negative (slanting away from the observer), balancing our converging and parallel displays in terms of the average absolute disparity subtended by the inducing surface patches.

Stereograms were constructed using *Strata-3D* software and setting the oversampling at four (allowing managing for sub-pixel disparity steps of 1/4). Each stereo pair was obtained by taking the projection of the entire 3D scene (both patches and the occluder) and rotating it around the vertical of half the convergence angle (1.55 deg, calculated for a viewing distance of 120 cm and an interocular distance of 6.5 cm). Within each subset of 3D relatable/nonrelatable displays, the pair of inducing planar surfaces could simulate (in the viewer centered coordinate system shown in Figure 5) any one of the 5 following slant magnitudes $\sigma = \pm 20, \pm 35, \pm 46, \pm 54, \pm 60$ deg. This means that, in Experiment 1, the *horizontal shear angle* of one monocular image of the patch relative to the other

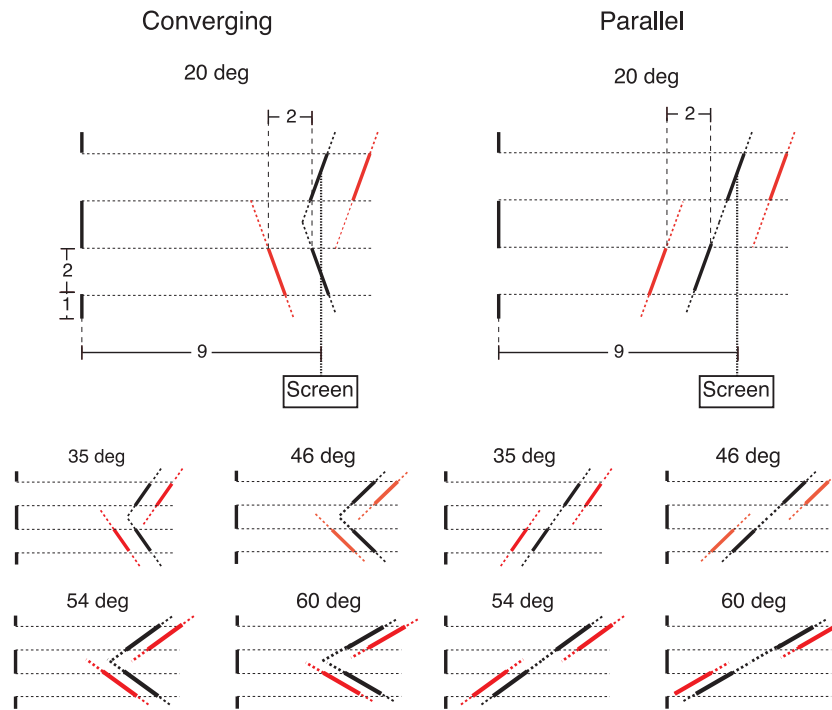


Figure 7. Geometry of experimental displays and simulated dimensions (taking as a reference size the aperture radius) over the 5 tested simulated slant values of the inducing surfaces for converging (left) and parallel (right) display types. The figure gives a simulated overhead/side view (depending on the experiment). The black lines to the left represent the occluder and the gaps in this line represent the apertures. Solid black slanted lines depict the 3D reference relatable condition while solid red slanted lines depict corresponding nonrelatable condition.

(necessary to simulate a surface with a vertical tilt direction) increased for each successive simulated slant condition of a constant 1.05 deg, ranging from 1.13 deg (when $\theta = \pm 20$) to 5.33 deg (when $\theta = \pm 60$ deg). In Experiment 2, the percent of horizontal compression of one image relative to the other (necessary to simulate a surface with a horizontal tilt direction) were as follows: 2%, 3.9%, 5.8%, 7.8%, and 9.8% (for $\theta = \pm 20$ to ± 60 deg, respectively).

Procedure

As shown in Figure 8, each speeded classification trial included the following:

1. a 30-pixel-wide red cross with a 9.1 arcmin disparity was displayed at the center of the screen;
2. when the observer was ready, he/she pressed a key to display the stimulus;
3. the display remained on the screen until one of the two response keys was pressed;
4. a 500-ms mask with zero horizontal disparity was displayed and the next trial followed.

Given individual variability in the time required to achieve a stereo percept, we felt it best to allow the observers to

control the stimulus duration, ending each presentation when they pressed the response key. However, to obtain meaningful response time data the observers were instructed to respond as quickly as possible.

The experiments were run in a dark room allowing for dark adaptation. The participant was seated in front of the CRT screen with his/her head stabilized by a chin rest maintaining the eyes at a constant distance (≈ 120 cm) from the screen. The procedure included instructions, training a test for slant perception, and the experimental session.

Instructions

The experimenter introduced binocular vision, told participants that the experiment involved slant perception (enabled via 3D goggles), and showed a physical model of the displays (two cardboard tabs with adjustable depth and slant attached to wires that extended through slits in two parallel walls viewed through two horizontally aligned holes cut into a flat piece of poster board that was placed in front of the two tabs). Instructions required participants to respond quickly and to use the cross to support steady fixation during stimulus presentation.

Training with experimental displays

All observers performed a session of 20 trials randomly selected from the set of experimental displays. On each

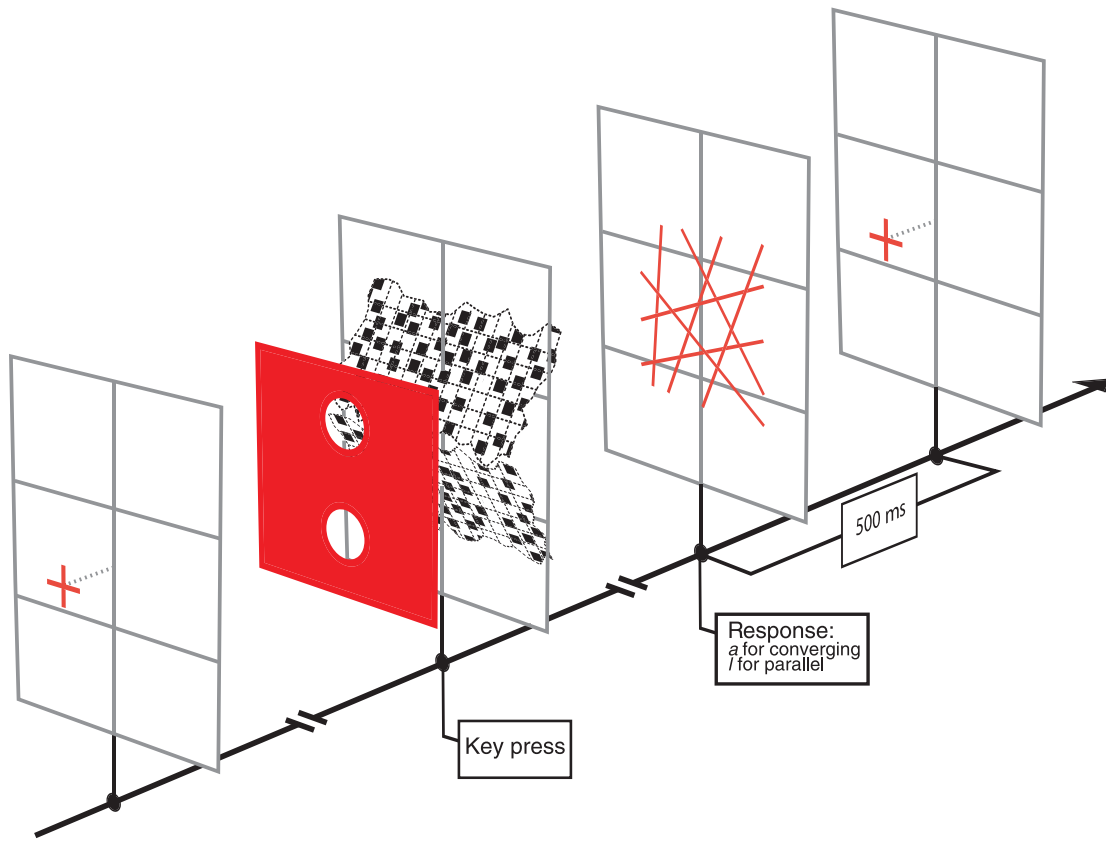


Figure 8. Temporal sequence used in the experiments. The illustration refers to a trial of Experiment 1 in which a converging 3D relatable display with aligned apertures was presented. Gray outlined rectangles depict the screen depth level (for each trial's event) together with three reference screen axes (the vertical and two horizontal axes whose heights on the screen match the one of apertures).

trial, participants were asked to verbalize what they perceived taking as much time as needed in giving their parallel/converging response. Each response was followed by auditory feedback.

Test for stereoscopic slant perception

Participants were screened for slant perception within two separate blocks of 20 trials each (supported by auditory feedback). Participants were required to respond following the standards of the experimental session. Only participants who at the end of the last block met performance criteria (60% correct and faster than 4 s) entered the experimental session.

Experimental session

The experimental session included the random presentation of 480 trials (without feedback), resulting from 12 repetitions of our 40 experimental displays. The 40 experimental displays resulted from the combination of 2 display types (converging, parallel) \times 5 inducing surface slant ($\theta = 20, 35, 46, 54, 60$ deg) \times 2 3D relatability conditions (3D relatable, nonrelatable) \times 2 alignment of the aperture pairs (aligned, misaligned). Other factors, such as the overall sign of slant of parallel displays, and the sign of depth shift, were counterbalanced across the trials. An experimental session took

nearly 70 minutes and was divided into 8 sessions (of 60 trials each) separated by short rest periods.

Analyses

Analyses were performed for sensitivity (d') and response time (RT) on correct classification responses for both display types (parallel, converging). These measures were comparable to those reported by Kellman, Garrigan, Shipley, Yin et al. (2005). Performance for displays with different overall sign of slant and for both possible depth shift directions were averaged for analysis. Sensitivity data were extracted by taking the converging displays as the positive target and the parallel displays as the negative target. A d' -prime was calculated for each unique combination of inducing surface slant value, relatability, and aperture alignment for a total of 20 unique d' -prime values per subject. Extremal d' -prime values (i.e., 100% performances) were corrected as a function of the number of trials for each experimental condition (maximal d' -prime value was 3.46). Only RTs for correct classification responses were analyzed. We further restricted analysis to correct responses that when normalized were inside of the $z = [\pm 1.96]$ bounds. For each subject, we obtained 40 mean RT values: one for each experimental display.

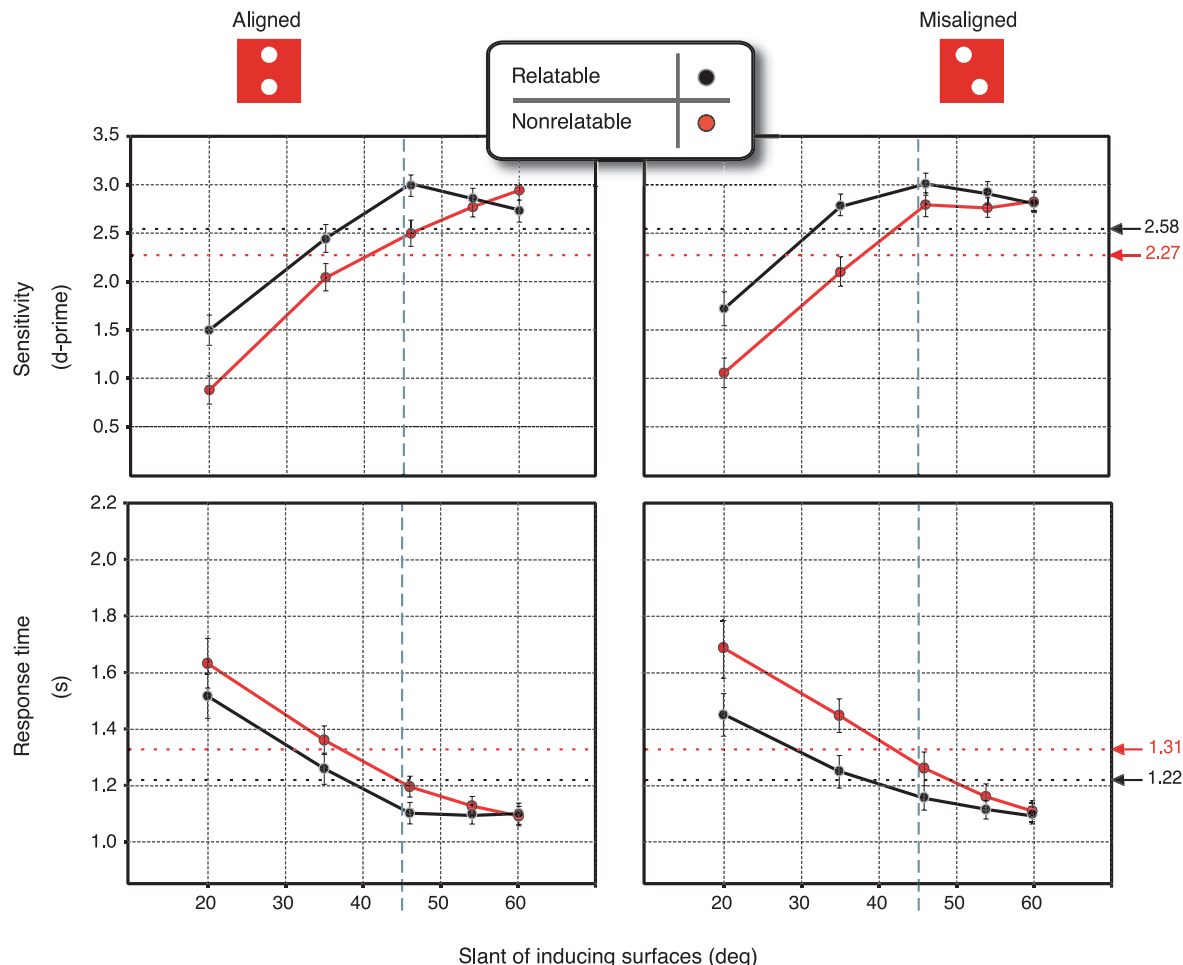


Figure 9. Speeded classification performance in Experiment 1. Top row: Mean sensitivity. Bottom row: Mean response time. Error bars show \pm one standard error of the mean. Data are shown for aligned (left) and misaligned (right) displays, for the five levels of absolute slant of inducers, and the two levels of 3D relatability (coded by color). The blue dotted line shows the limiting slant value over which (regardless of monotonicity) two converging planes may become nonrelatable (due to a violation of the 90-deg constraint).

Results of Experiment 1: Inducing surfaces with vertical tilt direction

Figure 9 depicts the sensitivity (top row) and mean RT collapsed over display types (bottom row). There was a clear effect of 3D relatability on both measures. Sensitivity was larger and RT was smaller in the 3D relatable relative to nonrelatable displays. Both d-prime and RT results show a strong improvement of performance with increasing slant of the inducing surfaces. No meaningful differences appeared between aligned vs. misaligned displays for either sensitivity or RT. Finally, the performance advantage due to 3D relatability decreased with increasing slant.

These observations were confirmed by the statistical analyses on d-prime and RT values. We analyzed d-primes in a 5 (inducing surface slant) \times 2 (3D relatability) \times 2 (apertures alignment) repeated measures ANOVA and RTs in a similar design with the addition of display type (parallel, converging) as a factor. The main effect of 3D relatability was significant for both d-prime ($F_{1, 25} = 20.96$,

$p < 0.001$) and RT ($F_{1, 25} = 20.52$, $p < 0.001$). The amount of increase in sensitivity due to 3D relatability was on the order of 0.31 (mean d-prime = 2.58 vs. 2.27 for 3D relatable vs. nonrelatable displays), which equated to 9% of our corrected d-prime scale. Similarly, the amount of reduction in the time needed to perform the classification task due to 3D relatability was of about 91 ms (mean RT = 1.22 vs. 1.31 s for 3D relatable vs. nonrelatable displays), equating to 7.2% of the global average RT of 1.26 s. The main effect of simulated slant of the inducing surfaces was also significant, with d-prime increasing ($F_{4, 100} = 184.5$, $p < 0.001$) and RT decreasing ($F_{4, 100} = 54.19$, $p < 0.0001$) as a function of simulated slant. There was no main effect for the alignment of aperture pairs for either d-prime or RT, consistent with the idea that the spread of surface qualities does not depend on particular aperture positions or their alignment relative to the direction of tilt of the inducing surfaces.

The surfaces slant \times 3D relatability interaction was significant for both d-prime ($F_{4, 92} = 10.4$, $p < 0.0001$) and

RTs ($F_{4, 92} = 5.22, p < 0.001$). A post-hoc analysis suggested that this effect was due to the decreasing differences between 3D relatable and nonrelatable displays at increasing slant values in a direction consistent with the effectiveness of the 90-deg constraint. Indeed the performance gain due to 3D relatability (difference between individual d-primes and individual RT for 3D relatable vs. nonrelatable displays) was significantly different from 0 only for values of inducing surface slant smaller than the limiting slant values of 45 deg beyond which a violation of the 90-deg constraint occurs. The d-prime gains for $\theta = 20, 35, 46, 54$, and 60 deg, respectively, were: 0.64 ($t_{25} = 5.2$, two tailed, $p < 0.001$), 0.54 ($t_{25} = 5.02$, two tailed, $p < 0.001$), 0.35 ($t_{25} = 3.10$, two tailed, $p < 0.005$), 0.13 ($t_{25} = 1.15$, two tailed, n.s.), and -0.11 ($t_{25} = -1.38$, two tailed, n.s.); while the RT gains were: -0.18 ($t_{25} = -3.8$, two tailed, $p < 0.001$), -0.15 ($t_{25} = -4.5$, two tailed, $p < 0.001$), -0.10 ($t_{25} = -3.4$, two tailed, $p < 0.005$), 0.03 ($t_{25} = -1.71$, two tailed, n.s.), and 0.00 ($t_{25} = 0.2$, two tailed, n.s.) s.

The effect of the display type on RT was not significant. However, the display type \times inducing surface slant interaction was significant ($F_{4, 100} = 4.32, p < 0.01$); RT decreased more steeply with increasing slant for converging displays than for parallel displays. This was confirmed by comparing changes in RT for displays with $\theta = 20$ vs. 60 deg for converging relative to parallel displays (0.58 vs. 0.35 s: $t_{25} = 2.5$, two tailed, $p < 0.05$). Finally, consistent with the idea that 3D relatability should affect converging display more than parallel displays over inducing surface slant conditions, a significant display type \times inducing surface slant \times 3D relatability interaction was found ($F_{4, 100} = 3.1, p < 0.05$).

Discussion

The results of Experiment 1 support the notion that visual interpolation includes surface-based processes independent of contour information and that these processes are geometrically constrained by the 3D positions and orientations of visible surface patches. The pattern of results substantially replicates that of Kellman, Garrigan, Shipley, Yin et al. (2005) for illusory contour displays, despite the lack of explicit bounding edges in our inducing surfaces. 3D relatability consistently affected speeded classification performance, by facilitating it for 3D relatable displays relative to displays in which 3D relatability was disrupted by both a depth shift of one surface relative to the other (violating the monotonicity constraint) and relative stereo slant (violating the 90-deg constraint in converging displays). These effects cannot be explained by slant sensitivity alone, given that relatable and nonrelatable displays determined different slant sensitivity/RT functions, producing the simulated slant/performance advantage trade-off predicted on the basis of a full effect of 3D relatability. Such a trade-off is unlikely

to depend on the different depth offset in relatable vs. nonrelatable displays, i.e., the *standing disparity* using the Gillam and Blackburn (1998) definition, for the following reasons: first, the expected effect should be constant over slant, given that the depth shift was always the same; second, Kellman, Garrigan, Shipley, Yin et al. (2005, Experiments 3 and 4) demonstrated that the classification advantage disappears when luminance-specified inducers with rounded edges hinder completion.

We suggest that, in general, the level of representation used by the visual system to connect fragmented images is inherently three-dimensional and not confined to the pictorial domain. This implies that 2D surface interpolation may constitute a special case of a more general 3D process. The other primary implication of these results is that such a representation is not based on contours alone; rather it includes surface-based features. More specifically, in our displays, disparity provides sufficient information for the extraction of the 3D orientation of inducing patches necessary to constrain surface interpolation: surface relations alone can provide 3D structure sufficient to produce connections of visible regions, or to preclude such connections.

The absence of any meaningful effect of aperture alignment further suggests that 3D surface interpolation depends on inducing surfaces' slant and their relative position in depth but not on their relative position in the image plane (as revealed by the apertures). The performance advantage was not affected by the spatial agreement between the direction of alignment and the direction of tilt of inducing surfaces. This behavior was not found for the completion of 3D contour-defined objects in Kellman, Garrigan, Shipley, Yin et al. (2005) as the performance advantages there were degraded by lateral misalignment of patches that (differently from our displays) necessarily involves a misalignment of inducing edges.

While the results of Experiment 1 provide strong support for a common geometry governing contour- and surface-based interpolation processes, they do not provide much information on the specific nature of the surface interpolation process. Experiment 1 addressed Aim #1 but not Aim #2 or #3. Experiment 2 addressed these latter two aims.

Results of Experiment 2: Inducing surfaces with horizontal tilt direction

As in Experiment 1, we analyzed mean sensitivity and RT. Figure 10 depicts these data for the 20 conditions of the experimental design, with mean d-prime in the top row and mean RT in the bottom row. Again, the distribution of data indicates the generality of 3D relatability constraints on surface completion. The key result is the similar condition interaction for d-prime and RT in Experiments 1 and 2. As in Experiment 1, speeded classification performance was hindered by the violation of the monotonicity

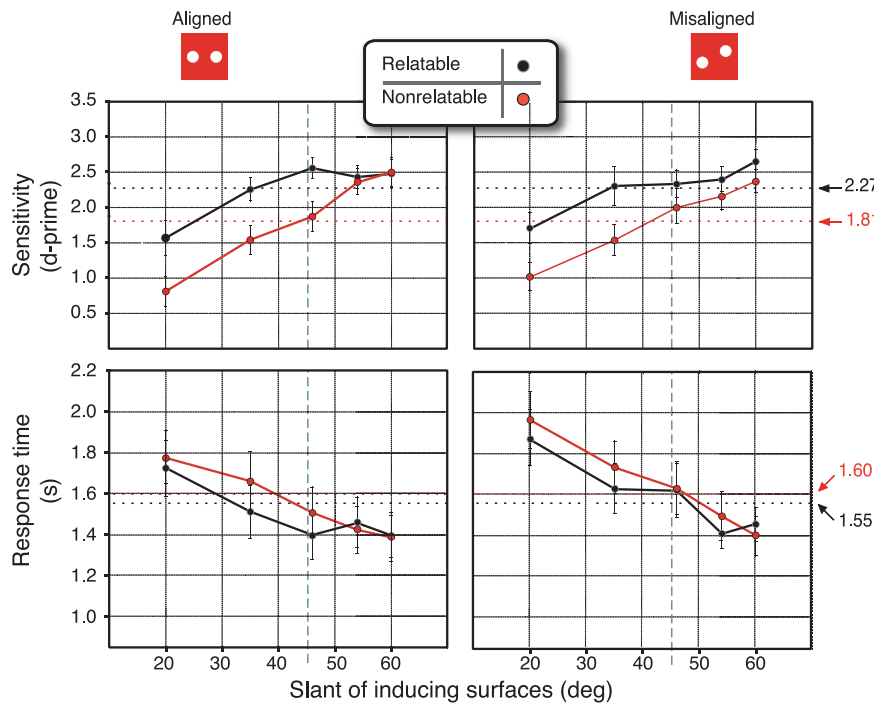


Figure 10. Speeded classification performance in Experiment 2. Top row: Mean sensitivity. Bottom row: Mean response time. Error bars show \pm one standard error of the mean. Data are shown for aligned (left) and misaligned (right) displays, for the five levels of absolute slant of inducers, and the two levels of 3D relatability (coded by color). The blue dotted line shows the limiting slant value over which (regardless of monotonicity) two converging planes become nonrelatable (due to violation of the 90-deg constraint).

constraint, leading to greater sensitivity for 3D relatable (2.27) vs. nonrelatable displays (1.81; with a 3D relatability advantage of about 13.2%) and faster RT (average RT was 1.54 and 1.60 s, respectively, with a 3D relatability advantage of about 3.5%). Performance was also hindered by violations of the 90-deg constraint, with reduced differences between 3D relatable and nonrelatable displays with increasing stereo slant of inducing surface patches. The data also reveal a slant anisotropy consistent with an overall lower sensitivity (average d-primes of 2.04 vs. 2.42 in Experiments 2 vs. 1, respectively) and lower speed of classification (average RT was 1.26 vs. 1.57 s in Experiments 1 vs. 2, respectively).

Overall, the pattern of RT was noisier in Experiment 2: response consistency (average individual variability of RT quantified by average s.e.m. values) was worse in Experiment 2 (0.13 s) than in Experiment 1 (0.06 s). To provide stronger evidence for the general conclusions relating the two experiments, we compared the patterns of d-prime and RT in Experiment 2 directly to those of Experiment 1: d-prime and RT were analyzed in a 2 (experiment) \times 5 (inducing surface slant) \times 2 (3D relatability) \times 2 (aperture alignment) mixed factorial ANOVA with experiment (i.e., global orientation) as a between-subjects variable. To optimize comparison with d-primes, we used RT collapsed over different types of display (parallel/converging), given the absence of a significant main effect of such a variable ($F_{1, 42} = 0.9$, n.s.).

The analysis revealed the following set of reliable effects on both sensitivity and RT: *experiment* (d-prime: $F_{1, 42} = 4.64$, $p < 0.05$; RT: $F_{1, 42} = 8.36$, $p < 0.01$), with an overall performance loss in Experiment 2 relative to Experiment 1; *3D relatability* (d-prime: $F_{1, 42} = 54.62$, $p < 0.001$; RT: $F_{1, 42} = 14.47$, $p < 0.001$), with an improved performance for relatable relative to nonrelatable displays; *inducing surface slant* (d-prime: $F_{4, 168} = 165.74$, $p < 0.001$; RT: $F_{4, 168} = 76.10$, $p < 0.001$) with increasing sensitivity and decreasing RT for increasing values of inducing surface slant; *inducing surface slant \times 3D relatability* (d-prime: $F_{4, 168} = 15.92$, $p < 0.001$; RT: $F_{4, 168} = 4.70$, $p < 0.005$), with the performance advantage due to 3D relatability decreasing for increasing values of slant.

No other reliable main effects or interactions were found for sensitivity, while the analysis on RT showed the following additional effects: *aperture alignment* ($F_{1, 42} = 10.22$, $p < 0.01$), with faster responses when the axis of alignment of the aperture pairs was in the same direction of the tilt of inducing surfaces (1.39 s), rather than when it was not (1.45 s); *aperture alignment \times 3D relatability* ($F_{4, 168} = 2.87$, $p < 0.05$) apparently due to an unexpected peak (more pronounced in Experiment 2) in the advantage for aligned over misaligned displays when the slant of inducing surfaces was 46 deg (1.30 vs. 1.43 s: $F_{1, 42} = 20.93$, $p < 0.001$). This result differs from other indications that aperture alignment had little influence on surface interpolation.

Discussion

Experiment 2 aimed to answer two basic questions:

1. Is the 3D relatability effect found in Experiment 1 independent of the orientation of the inducing surfaces (supporting the isotropicity of the unit formation process at the surface level)?
2. Is classification performance, on average, weakened by inducing surfaces with a vertical rather than a horizontal tilt direction (supporting an anisotropic computation of inducing surface orientation)?

In general, the results of Experiment 2 taken together with those of Experiment 1 support a positive answer to both questions. The data trends obtained in Experiment 2 were similar to those of Experiment 1 (with the exception of a questionable main effect of aperture alignment on RT), despite the fact that in this second experiment the tilt of inducing surface patches was horizontal leading to poorer overall d-prime, RT, and response consistency relative to Experiment 1. These findings support the idea that visual interpolation occurs between inducing surfaces even in the absence of explicit contour information, and that the surface interpolation process is likely to be *isotropic* (as supported by the absence of any interaction of the *experiment* factor with other factors) and geometrically constrained by the 3D relatability of surface patches (as supported by the consistent 3D relatability advantage). The extraction of 3D position and orientation of inducers is, in contrast, anisotropic likely consisting of a reduced effectiveness of surfaces with horizontal vs. vertical tilt as inducers of a 3D percept, as supported by the overall performance loss of Experiment 2 producing a significant effect of the *experiment* factor.

Conclusions

We reported two experiments on surface interpolation and 3D relatability, demonstrating that visual interpolation is geometrically constrained even when explicit edge information is absent, and that 3D contour and surface interpolation share common geometric constraints as formalized by 3D relatability (Kellman, Garrigan, & Shipley, 2005). When the simulated stereo slant and position in depth of two unbounded surface patches (as revealed by apertures in an occluder) satisfy 3D relatability constraints, their relative spatial orientations (parallel vs. converging) produce superior classification performance in an objective task, compared to cases in which their spatial relations violate 3D relatability. This pattern of results converges with that found by Kellman, Garrigan, Shipley, Yin et al. (2005), although they used bounded (rather than unbounded) planar surfaces. 3D relatability appears to be a general constraint formalizing the geo-

metric relations needed to perceptually connect any pair of visual fragments regardless of their specification (being at the level of contours, surfaces, or both). This idea is consistent with recent findings on the generality of relatability in which its efficacy have been shown even for motion signals of small Gabor patches (Bex, Simmers, & Dakin, 2001) and dot-motion patches (Hess & Ledgeray, 2003; Ledgeray & Hess, 2002).

The performance advantage for relatable surface patches suggests an important constraint on processes that produce unitary 3D surface representations from fragmentary input: *explicit edges are not required for 3D surface interpolation*. In the absence of contours, interpolation is geometrically constrained by the spatial positions and orientations of inducing surface patches as specified in the image by information extracted from projected surface markings (i.e., disparity). In this regard, the relevant orientation parameter is the slant of the inducing surfaces: the performance advantage did not much depend on the relative position in the image plane of inducers (as revealed by apertures) and on their alignment relative to the tilt direction of inducing surface. It is likely that surface spreading, constrained by 3D orientation information, occurs behind occluders in all directions.

Facilitation patterns were also not influenced by the global 3D orientation of the inducing surface patches, occurring both in Experiment 1 (where they appeared with a vertical direction of tilt) and in Experiment 2 (where they appeared with a horizontal direction of tilt). This result suggests an isotropic unit formation process. The outcome is consistent with a previous study by Saidpour et al. (1994) on the interpolation across surfaces in structure from motion where the smoothness of the interpolated surface was found to be independent of the direction of tilt of inducing surfaces (vertical or horizontal).

The reduced sensitivity and classification speed found in Experiment 2, relative to Experiment 1, say something interesting about the base input for early processing involved in surface interpolation. The effectiveness of a surface patch as inducer of a 3D percept depends on its global orientation, being reduced when patches are tilted in horizontal relative to vertical directions. Following classic work on slant anisotropy (Caganello & Rogers, 1988, 1993; Gillam & Ryan, 1992; Mitchison & McKee, 1990; Rogers & Graham, 1983), we interpreted this result as showing that, in our displays, higher order disparity (rather than the positional disparity) of corresponding groups of dots provides key information for a direct specification (rather than an indirect reconstruction) of the 3D orientation of inducing patches necessary to constrain surface interpolation.

To our knowledge, our work provides the first evidence that explicitly disentangles 3D surface from contour interpolation. Our displays were designed to reveal geometric constraints at the surface level alone, providing important insights on the possible relationship between 3D contour and 3D surface interpolation. One possibility is

that 3D contour and 3D surface interpolation are distinct processes that follow similar geometric constraints. The other possibility is that 3D surface and contour interpolation could be more intrinsically connected. The idea that surfaces spread up to real or interpolated boundaries (Grossberg & Mingolla, 1985; Yin et al., 1997) could be one aspect of a more complex, multi-tiered procedure where contour and surface interpolation are self-sufficient processes that can interact and cooperate. Kellman, Garrigan, and Shipley (2005, see Figure 10) presented a display in which contours were collinear but were part of mismatched surfaces; this display appeared to contain two disconnected visible regions, consistent with the possibility that in 3D, contours may interpolate only when there is sufficient geometric compatibility of the surfaces of which the contours are part. This issue is an important one for future research.

The present results offer an initial characterization of the geometry of 3D surface interpolation and in general highlight the importance of surface processes in object formation. It has sometimes been claimed that work on contour interpolation implies a neglect of surface processes (Anderson, 2007; but see Kellman, Garrigan, Shipley, & Keane, 2007). Our work has long recognized the importance of complementary contour and surface processes (Kellman, 2003; Kellman & Shipley, 1991; Yin et al., 1997, 2000). The present results, however, offer the first evidence that surface interpolation in 3D is governed by relatability constraints similar to those operating in contour interpolation. These results occurred under conditions in which contours were lacking but other sources of information indicated the perceived positions and orientations of visual fragments. Our findings, together with most recent findings in 2D (Albert, 2007; Fulvio et al., 2008), 3D (Kellman, Garrigan, & Shipley, 2005), and spatio-temporal (Palmer, Kellman, & Shipley, 2006) completion, indicate that across a variety of contexts the common geometry of relatability determines which visible fragments may be connected to form objects.

Applied mathematics, computational theory, and research in human vision have provided several algorithms for the extraction of 3D planar surface orientations from image projections as well as for the interpolation of visual fragments (Elder & Goldberg, 2002; Fantoni & Gerbino, 2003; Guy & Medioni, 1996; Horn, 1981; Kass, Witkin, & Terzopoulos, 1987; Kubovy & Gepshtain, 2000; Mumford, 1994; Ullman, 1976; Williams & Jacobs, 1997). Few efforts have combined interpolation with 3D information and, with the exception of Grimson (1981), it has remained unclear how long-range completions under occlusion might occur even when explicit edges are missing in the image (as in our displays). Our results are consistent with a model including:

1. an algorithm for the extraction of inducing surface orientations and positions from the higher order disparity arrangements present in the image;

2. a geometric module determining the occurrence and strength of visual completion based on the degree of fulfillment of 3D relatability constraints; and
3. an algorithm for the generation of interpolated surfaces smoothly connecting pairs of 3D relatable inducing surface patches.

Otherwise, the visual system could just run the interpolation stage, which might fail to provide useful results when fragment geometry violates relatability. One way to distinguish between such possibilities would be a test for scale invariance. From a computational perspective, the geometric module could be conceived as a coarse and cheap filter leading to a stable interpolation over scale variations, allowing relatability to hold over different distances between the patches. Different predictions should apply in the absence of the coarse filter, where completions over small and large distance scales should lead to somewhat different shapes (Gerbino & Fantoni, 2006). Although our experiments cannot provide information on scale invariance (since they involved only one intermediate scale level), the question is ripe for further studies: for instance, through testing the effects of viewing distance and different combinations of patch positions.

Yet to be determined is whether surface interpolation utilizes spatial position and orientation information that are determined from a variety of information sources. As hypothesized by Kellman, Garrigan, and Shipley (2005) this would imply the contribution from later neural areas than V1 or V2 (although these areas have been claimed to be relevant to static, 2D interpolation), such as cIPS (caudal intraparietal sulcus), which has been found to be involved in the representation of 3D slant obtained from multiple sources of spatial information (e.g., Sakata, Taira, Kusunoki, Murata, & Tanaka, 1997).

We hope that accumulating evidence about the constraints on and determinants of visual interpolation will not only advance computational models but will help produce a more comprehensive understanding of neural structures that allow perceivers to compute coherent objects and surfaces from fragmentary input.

Acknowledgments

The authors gratefully acknowledge supports from the US National Eye Institute Grant EY13518 to PJK, Grant PRIN 2005119851 to WG, Fulbright (CIES) Award to CF.

Commercial relationships: none.

Corresponding author: Carlo Fantoni.

Email: fantoni@psico.units.it; carlo.fantoni@iit.it.

Address: Department of Psychology and B.R.A.I.N. Center for Neuroscience, University of Trieste, via Sant'Anastasio 12, 34134 Trieste, Italy.

References

- Albert, M. K. (2001). Surface perception and the generic view principle. *Trends in Cognitive Sciences*, 5, 197–203. [PubMed]
- Albert, M. K. (2007). Mechanisms of modal and amodal interpolation. *Psychological Review*, 114, 455–469. [PubMed]
- Anderson, B. L. (2007). Filling-in models of completion: Rejoinder to Kellman, Garrigan, Shipley, and Keane (2007) and Albert (2007). *Psychological Review*, 114, 509–527. [PubMed]
- Bakin, J. S., Nakayama, K., & Gilbert, C. D. (2000). Visual responses in monkey areas V1 and V2 to three-dimensional surface configurations. *Journal of Neuroscience*, 20, 8188–8198. [PubMed]
- Baylis, G. C., & Driver, J. (1993). Visual attention and objects: Evidence for hierarchical coding of location. *Journal of Experimental Psychology: Human Perception and Performance*, 19, 451–470. [PubMed]
- Behrmann, M., Zemel, R. S., & Mozer, M. C. (1998). Object-based attention and occlusion: Evidence from normal participants and a computational model. *Journal of Experimental Psychology: Human Perception and Performance*, 24, 1011–1036. [PubMed]
- Bertamini, M. (2001). The importance of being convex: An advantage for convexity when judging position. *Perception*, 30, 1295–1310. [PubMed]
- Bex, P. J., Simmers, A. J., & Dakin, S. C. (2001). Snakes and ladders: The role of temporal modulation in visual contour integration. *Vision Research*, 41, 3775–3782. [PubMed]
- Blake, A., & Zisserman, A. (1987). *Visual reconstruction*. Cambridge, MA: MIT Press.
- Blakemore, C. (1970). A new kind of stereoscopic vision. *Vision Research*, 10, 1181–1199. [PubMed]
- Bradshaw, M. F., & Rogers, B. J. (1993). Sensitivity to horizontally and vertically oriented stereoscopic corrugations as a function of corrugation frequency. *Perception*, 22, 117.
- Braunstein, M. L. (1968). Motion and texture as sources of slant information. *Journal of Experimental Psychology*, 78, 247–253. [PubMed]
- Caganello, R., & Rogers, B. J. (1993). Anisotropies in the perception of stereoscopic surfaces: The role of orientation disparity. *Vision Research*, 33, 2189–2201. [PubMed]
- Caganello, R. B., & Rogers, B. J. (1988). Local orientation differences affect the perceived slant of stereoscopic surfaces. *Investigative Ophthalmology & Visual Science*, 29, 399.
- Cornilleau-Pérès, V., & Droulez, J. (1989). Visual perception of surface curvature: Psychophysics of curvature detection induced by motion parallax. *Perception & Psychophysics*, 46, 351–364. [PubMed]
- de Vries, S. C., Kappers, A. M., & Koenderink, J. J. (1993). Shape from stereo: A systematic approach using quadratic surfaces. *Perception & Psychophysics*, 53, 71–80. [PubMed]
- de Vries, S. C., Kappers, A. M., & Koenderink, J. J. (1994). Influence of surface attitude and curvature scaling on discrimination of binocularly presented curved surfaces. *Vision Research*, 34, 2409–2423. [PubMed]
- Domini, F., & Caudek, C. (2003). 3-D structure perceived from dynamic information: A new theory. *Trends in Cognitive Sciences*, 7, 444–449. [PubMed]
- Duncan, J. (1984). Selective attention and the organization of visual information. *Journal of Experimental Psychology: General*, 113, 501–517. [PubMed]
- Elder, J. H., & Goldberg, R. M. (2002). Ecological statistics of Gestalt laws for the perceptual organization of contours. *Journal of Vision*, 2(4):5, 324–353, <http://journalofvision.org/2/4/5/>, doi:10.1167/2.4.5. [PubMed] [Article]
- Fantoni, C., Bertamini, M., & Gerbino, W. (2005). Contour curvature polarity and surface interpolation. *Vision Research*, 45, 1047–1062. [PubMed]
- Fantoni, C., & Gerbino, W. (2003). Contour interpolation by vector-field combination. *Journal of Vision*, 3(4):4, 281–303, <http://journalofvision.org/3/4/4/>, doi:10.1167/3.4.4. [PubMed] [Article]
- Fantoni, C., & Gerbino, W. (2006). 3D surface orientation based on orientation disparity alone [Abstract]. *Journal of Vision*, 6(6):645, 645a, <http://journalofvision.org/6/6/645/>, doi:10.1167/6.6.645.
- Fantoni, C., Hilger, J. D., Gerbino, W., & Kellman, P. J. (2005). Surface interpolation and 3D relatability [Abstract]. *Journal of Vision*, 5(8):341, 341a, <http://journalofvision.org/5/8/341/>, doi:10.1167/5.8.341.
- Field, D. J., Hayes, A., & Hess, R. F. (1993). Contour integration by the human visual system: Evidence for a local “association field.” *Vision Research*, 33, 173–193. [PubMed]
- Fiorani, M., Jr., Rosa, M. G., Gattas, R., & Rocha-Miranda, C. E. (1992). Dynamic surrounds of receptive fields in primate striate cortex: A physiological basis for perceptual completion? *Proceedings of the National Academy of Science of the United States of America*, 89, 8547–8551. [PubMed]
- Fulvio, J. M., Singh, M., & Maloney, L. T. (2008). Precision and consistency of contour interpolation. *Vision Research*, 48, 831–849. [PubMed]

- Gårding, J., Porrill, J., Mayhew, J. E., & Frisby, J. P. (1995). Stereopsis, vertical disparity and relief transformations. *Vision Research*, 35, 703–722. [PubMed]
- Geisler, W. S., Perry, J. S., Super, B. J., & Gallogly, D. P. (2001). Edge co-occurrence in natural images predicts contour grouping performance. *Vision Research*, 41, 711–724. [PubMed]
- Gerbino, W., & Fantoni, C. (2006). Visual interpolation is not scale invariant. *Vision Research*, 46, 3142–3159. [PubMed]
- Gibson, J. J. (1950). *The perception of visual world*. Boston: Houghton Mifflin.
- Gibson, J. J. (1979). *The ecological approach to visual perception*. Boston: Houghton Mifflin.
- Gillam, B. J., & Blackburn, S. G. (1998). Surface separation decreases stereoscopic slant but a monocular aperture increases it. *Perception*, 27, 1267–1286. [PubMed]
- Gillam, B., Flagg, T., & Finlay, D. (1984). Evidence for disparity change as the primary stimulus for stereoscopic processing. *Perception & Psychophysics*, 36, 559–564. [PubMed]
- Gillam, B., & Ryan, C. (1992). Perspective, orientation disparity, and anisotropy in stereoscopic slant perception. *Perception*, 21, 427–439. [PubMed]
- Gold, J. M., Murray, R. F., Bennett, P. J., & Sekuler, A. B. (2000). Deriving behavioral receptive fields for visually completed contours. *Current Biology*, 10, 663–666. [PubMed]
- Grimson, W. E. (1981). A computer implementation of a theory of human stereo vision. *Philosophical Transactions of the Royal Society of London B: Biological Sciences*, 292, 217–253. [PubMed]
- Grossberg, S., & Mingolla, E. (1985). Neural dynamics of form perception: Boundary completion, illusory figures, and neon color spreading. *Psychological Review*, 92, 173–211. [PubMed]
- Guttman, S. E., Sekuler, A. B., & Kellman, P. J. (2003). Temporal variations in visual completion: A reflection of spatial limits? *Journal of Experimental Psychology: Human Perception & Performance*, 29, 1211–1227. [PubMed]
- Guy, G., & Medioni, G. (1996). Inferring global perceptual contours from local features. *International Journal of Computer Vision*, 20, 113–133.
- Harris, M., Freeman, T., & Hughes, J. (1992). Retinal speed gradients and the perception of surface slant. *Vision Research*, 32, 587–590. [PubMed]
- Heitger, F., Rosenthaler, L., von der Heydt, R., Peterhans, E., & Kübler, O. (1992). Simulation of neural contour mechanisms: From simple to end-stopped cells. *Vision Research*, 32, 963–981. [PubMed]
- Heitger, F., von der Heydt, R., Peterhans, E., Rosenthaler, L., & Kubler, O. (1998). Simulation of neural contour mechanisms: Representing anomalous contours. *Image and Vision Computing*, 16, 407–421.
- Hess, R. F., & Ledgeway, T. (2003). The detection of direction-defined and speed defined spatial contours: One mechanism or two? *Vision Research*, 43, 597–606. [PubMed]
- Hilger, J. D., Fantoni, C., Gerbino, W., & Kellman, P. J. (2006). Surface interpolation and slant anisotropy [Abstract]. *Journal of Vision*, 6(6):334, 334a, <http://journalofvision.org/6/6/334/>, doi:10.1167/6.6.334.
- Hoffman, D. D., & Richards, W. A. (1984). Parts of recognition. *Cognition*, 18, 65–96. [Also published as MIT AI Memo 732, 1983; In S. Pinker (Ed.), *Visual Cognition*, <http://mitpress.mit.edu/>. MIT Press, 1985; In A. Pentland (Ed.), *From Pixels to Predicates: Recent Advances in Computational Vision*, Ablex Publishing Company, 1986; and In M. Fischler & O. Firschein (Eds.), *Readings in Computer Vision*, Morgan & Kaufmann Publishers, 1987.]
- Horn, B. K. P. (1981). *The curve of least energy*. Cambridge: MIT Press.
- Howard, I. P., & Kaneko, H. (1994). Relative shear disparities and the perception of surface inclination. *Vision Research*, 34, 2505–2517. [PubMed]
- Jones, D. G., & Malik, J. (1991). *Determining three-dimensional shape from orientation and spatial frequency disparities II—Using corresponding image patches*. Computer Science Division, University of California Berkeley. Technical Report No. UCB-CSD, 91–657.
- Kanizsa, G. (1979). *Organization in vision*. New York: Praeger.
- Kapadia, M. K., Ito, M., Gilbert, C. D., & Westheimer, G. (1995). Improvements in visual sensitivity by changes in local context: Parallel studies in human observers and in V1 of alert monkeys. *Neuron*, 15, 843–856. [PubMed]
- Kass, M., Witkin, A., & Terzopoulos, D. (1987). Snakes: Active minimum energy seeking contours. In *Proceedings of the First International Conference on Computer Vision (ICCV)* (pp. 259–268).
- Kellman, P. J. (2003). Segmentation and grouping in object perception: A four-dimensional approach. In M. Behrmann, R. Kimchi, & C. R. Olson (Eds.), *Perceptual organization in vision: Behavioral and neural perspectives* (pp. 155–201). Hillsdale, NJ: Erlbaum.
- Kellman, P. J., Garrigan, P., & Shipley, T. F. (2005). Object interpolation in three dimensions. *Psychological Review*, 112, 586–609. [PubMed]

- Kellman, P. J., Garrigan, P., Shipley, T. F., & Keane, B. P. (2007). Postscript: Identity and constraints in, models of object formation. *Psychological Review*, 114, 502–508.
- Kellman, P. J., Garrigan, P., Shipley, T. F., Yin, C., & Machado, L. (2005). 3-D interpolation in object perception: Evidence from an objective performance paradigm. *Journal of Experimental Psychology: Human Perception and Performance*, 31, 558–583. [PubMed]
- Kellman, P. J., Guttman, S. E., & Wickens, T. D. (2001). Geometric and neural models of object perception. In T. F. Shipley & P. J. Kellman (Eds.). *From fragments to objects: Segmentation and grouping in vision* (vol. 130, pp. 181–246) (Chapter 7). Oxford, UK: Elsevier Science.
- Kellman, P. J., & Shipley, T. F. (1991). A theory of visual interpolation in object perception. *Cognitive Psychology*, 23, 141–221. [PubMed]
- Knill, D. C. (1992). Perception of surface contours and surface shape: From computation to psychophysics. *Journal of the Optical Society of America*, 9, 1449–1464. [PubMed]
- Koenderink, J. J., & van Doorn, A. J. (1976). Geometry of binocular vision and a model for stereopsis. *Biological Cybernetics*, 21, 29–35. [PubMed]
- Koffka, K. (1935). *Principles of gestalt psychology*. New York: Harcourt Brace.
- Kramer, A. F., & Watson, S. E. (1996). Object-based visual selection and the principle of uniform connectedness. In A. Kramer, M. Coles, & G. Logan (Eds.), *Converging operations in the study of visual selective attention* (pp. 395–414). Washington, D.C.: American Psychological Association.
- Kubovy, M., & Gepshtein, S. (2000). Optimal curvatures in the completion of visual contours. *Investigative Ophthalmology and Visual Science*, 41, B568.
- Ledgeway, T., & Hess, R. F. (2002). Rules for combining the outputs of local motion detectors to define simple contours. *Vision Research*, 42, 653–659. [PubMed]
- Li, C. Y., & Li, W. (1994). Extensive integration field beyond the classical receptive field of cat's striate cortical neurons—Classification and tuning properties. *Vision Research*, 34, 2337–2355. [PubMed]
- Li, G., & Zucker, S. W. (2005). Stereo for slanted surfaces: First order disparities and normal consistency. In *Proceedings of EMMCVPR, LNCS 3757* (pp. 617–632).
- Liu, B., & Todd, J. T. (2004). Perceptual biases in the interpretation of 3D shape from shading. *Vision Research*, 44, 2135–2145. [PubMed]
- Malik, J., & Rosenholtz, R. (1997). Computing local surface orientation and shape from texture for curved surfaces. *International Journal of Computer Vision*, 23, 149–168.
- Marr, D. (1982). *Vision*. San Francisco: Freeman.
- Marr, D., & Poggio, T. (1979). A computational theory of human stereo vision. *Proceedings of the Royal Society of London B: Biological Sciences*, 204, 301–328. [PubMed]
- Mayhew, J. E., & Longuet-Higgins, H. C. (1982). A computational model of binocular depth perception. *Nature*, 297, 376–378. [PubMed]
- Metzger, W. (1954). *Psychologie*. Steinkopff (1st ed., 1941). Spanish translation: *Psicología*, 1954, Editorial Nova. Italian translation: *I fondamenti della psicologia della Gestalt*, 1963, Firenze, Giunti-Barbera.
- Michotte, A., Thinès, G., & Crabbé, G. (1964). *Les compléments amodaux des structures perpectives*. Louvain: Publications Universitaires.
- Mitchison, G. J., & McKee, S. P. (1990). Mechanisms underlying the anisotropy of stereoscopic tilt perception. *Vision Research*, 30, 1781–1791. [PubMed]
- Moore, C., & Engel, S. A. (2001). Neural response to perception of volume in the lateral occipital complex. *Neuron*, 29, 277–286. [PubMed]
- Mumford, D. (1994). Elastica and computer vision. In C. Bajaj (Ed.), *Algebraic geometry and its applications* (pp. 491–506). New York: Springer-Verlag.
- Murray, M. M., Foxe, D. M., Javitt, D. C., & Foxe, J. J. (2004). Setting boundaries: Brain dynamics of modal and amodal illusory shape completion in humans. *Journal of Neuroscience*, 24, 6898–6903. [PubMed]
- Nakayama, K., Shimojo, S., & Silverman, G. H. (1989). Stereoscopic depth: Its relation to image segmentation, grouping, and the recognition of occluded objects. *Perception*, 18, 55–68. [PubMed]
- Nguyenkim, J. D., & DeAngelis, G. C. (2003). Disparity-based coding of three-dimensional surface orientation by macaque middle temporal neurons. *Journal of Neuroscience*, 23, 7117–7128. [PubMed]
- Norman, J. F., & Lappin, J. S. (1992). The detection of surface curvatures defined by optical motion. *Perception & Psychophysics*, 51, 386–396. [PubMed]
- Palmer, E. M., Kellman, P. J., & Shipley, T. F. (2006). A theory of dynamic occluded and illusory object perception. *Journal of Experimental Psychology: General*, 135, 513–541. [PubMed]
- Pelli, D. G. (1997). The VideoToolbox software for visual psychophysics: Transforming numbers into movies. *Spatial Vision*, 10, 437–442. [PubMed]
- Ringach, D. L., & Shapley, R. (1996). Spatial and temporal properties of illusory contours and amodal boundary

- completion. *Vision Research*, 36, 3037–3050. [PubMed]
- Rogers, B. J., & Graham, M. E. (1983). Anisotropies in the perception of three-dimensional surfaces. *Science*, 221, 1409–1411. [PubMed]
- Saidpour, A., Braunstein, M. L., & Hoffman, D. D. (1992). Interpolation in structure from motion. *Perception & Psychophysics*, 51, 105–117. [PubMed]
- Saidpour, A., Braunstein, M. L., & Hoffman, D. D. (1994). Interpolation across surface discontinuities in structure-from-motion. *Perception & Psychophysics*, 55, 611–622. [PubMed]
- Sakata, H., Taira, M., Kusunoki, M., Murata, A., & Tanaka, Y. (1997). The TINS Lecture. The parietal association cortex in depth perception and visual control of hand action. *Trends in Neuroscience*, 20, 350–357. [PubMed]
- Sekuler, A. B., Palmer, S. E., & Flynn, C. (1994). Local and global processes in visual completion. *Psychological Science*, 5, 260–267.
- Singh, M., & Hoffman, D. D. (1999). Completing visual contours: The relationship between relatability and minimizing inflections. *Perception & Psychophysics*, 61, 943–951. [PubMed]
- Stevens, K. A. (1981). The visual interpretation of surface contours. *Artificial Intelligence*, 17, 47–73.
- Stevens, K. A. (1983). Slant-tilt: The visual encoding of surface orientation. *Biological Cybernetics*, 46, 183–195. [PubMed]
- Takeichi, H., Nakazawa, H., Murakami, I., & Shimojo, S. (1995). The theory of curvature constraint line for amodal completion. *Perception*, 24, 373–389. [PubMed]
- Terzopoulos, D. (1986). Regularization of inverse problems involving discontinuities. *IEEE Transactions on Pattern Analysis and Machine Intelligence*, 4, 413–424.
- Tse, P. U., & Albert, M. K. (1998). Amodal completion in the absence of image tangent discontinuities. *Perception*, 27, 455–464. [PubMed]
- Tyler, C. W., & Sutter, E. E. (1979). Depth from spatial frequency difference: An old kind of stereopsis? *Vision Research*, 19, 859–865. [PubMed]
- Ullman, S. (1976). Filling-in the gaps: The shape of subjective contours and a model for their generation. *Biological Cybernetics*, 25, 1–6.
- van Ee, R., & Erkelens, C. J. (1995). Binocular perception of slant about oblique axes relative to a visual frame of reference. *Perception*, 24, 299–314. [PubMed]
- van Ee, R., & Erkelens, C. J. (1998). Temporal aspects of binocular slant perception: An evaluation and extension of Howard and Kaneko's theory. *Vision Research*, 38, 3871–3882. [PubMed]
- Wallach, H., & Bacon, J. (1976). Two forms of retinal disparity. *Perception & Psychophysics*, 19, 375–382.
- Wildes, R. P. (1991). Direct recovery of three-dimensional scene geometry from binocular stereo disparity. *IEEE Transaction on Pattern Analysis and Machine Intelligence*, 13, 761–774.
- Williams, L. R., & Jacobs, D. W. (1997). Stochastic completion fields: A neural model of illusory contour shape and salience. *Neural Computation*, 9, 837–858. [PubMed]
- Yin, C., Kellman, P. J., & Shipley, T. F. (1997). Surface completion complements boundary interpolation in the visual integration of partly occluded objects. *Perception*, 26, 1459–1479. [PubMed]
- Yin, C., Kellman, P. J., & Shipley, T. F. (2000). Surface integration influences depth discrimination. *Vision Research*, 40, 1969–1978. [PubMed]